HHS Public Access

Author manuscript

J Control Release. Author manuscript; available in PMC 2019 March 28.

Published in final edited form as:

J Control Release. 2018 March 28; 274: 69–80. doi:10.1016/j.jconrel.2018.01.020.

Inhibiting Intimal Hyperplasia in Prosthetic Vascular Grafts via Immobilized All-trans Retinoic Acid

Elaine K. Gregory[1,3], **Antonio Webb**[4], **Janet M. Vercammen**[1,3], **Megan E. Kelly**[1,3], **Banu Akar**[2], **Robert van Lith**[2,3], **Edward M. Bahnson**[5], **Wulin Jiang**[1,3], **Guillermo A. Ameer**[1,2,3,**], and **Melina R. Kibbe**[1,3,5,**]

[1]Department of Surgery, Northwestern University Feinberg School of Medicine, Chicago, IL 60611

[2]Biomedical Engineering Department, McCormick School of Engineering, Northwestern University, Evanston, IL 60201

[3]Simpson Querrey Institute for BioNanotechnology, Northwestern University, Chicago, IL 60611

[4]The University of Florida, Gainesville, FL 32611

[5]Department of Surgery, University of North Carolina at Chapel Hill, Chapel Hill, NC 27599

Abstract

Peripheral arterial disease is a leading cause of morbidity and mortality. The most commonly utilized prosthetic material for peripheral bypass grafting is expanded polytetrafluoroethylene (ePTFE) yet it continues to exhibit poor performance from restenosis due to neointimal hyperplasia, especially in femoral distal bypass procedures. Recently, we demonstrated that periadventitial delivery of all-trans retinoic acid (atRA) immobilized throughout porous poly(1,8 octamethylene citrate) (POC) membranes inhibited neointimal formation in a rat arterial injury model. Thus, the objective of this study was to investigate whether atRA immobilized throughout the lumen of ePTFE vascular grafts would inhibit intimal formation following arterial bypass grafting. Utilizing standard ePTFE two types of atRA-containing ePTFE vascular grafts were fabricated and evaluated: grafts whereby all-trans retinoic acid was directly immobilized on ePTFE (atRA-ePTFE) and grafts where all-trans retinoic acid was immobilized onto ePTFE grafts coated with POC (atRA-POC-ePTFE). All grafts were characterized by SEM, HPLC, and FTIR

Address for Correspondence: Melina R Kibbe, MD, Department of Surgery4041 Burnett Womack, 101 Manning Drive, Chapel Hill, NC 27599-7050, Tel: 919-966-4320, melina_kibbe@med.unc.edu.

**Authors share senior authorship.

DISCLOSURES

Drs. Ameer, Webb, and Kibbe have ownership interests in VesselTek BioMedical LLC, the recipient of grant 1R43HL096217-01A1. Drs. Ameer, Webb, and Kibbe are listed as inventors on patent applications related to this work that were submitted by Northwestern University and VesselTek BioMedical LLC.

Author Contributions: EKG, AW, JMV, MEK, RV, EMB, WJ, BA, GAA and MRK participated in data collection and/or data analysis; EKG drafted the manuscript; EKG, AW, JMV, RV, BA, EMB, GAA and MRK edited and revised the manuscript; EKG, EMB, GAA, and MRK approved final version of manuscript; GAA and MRK secured funding for the project.

and physical chararcteristics were evaluated in vitro. Modification of these grafts, did not significantly alter their physical characteristics or biocompatibility, and resulted in inhibition of intimal formation in a rat aortic bypass model, with atRA-POC-ePTFE inhibiting intimal formation at both the proximal and distal graft sections. In addition, treatment with atRA-POC-ePTFE resulted in increased graft endothelialization and decreased inflammation when compared to the other treatment groups. This work further confirms the biocompatibility and efficacy of locally delivered atRA to inhibit intimal formation in a bypass setting. Thus, atRA-POC-ePTFE grafts have the potential to improve patency rates in small diameter bypass grafts and warrant further investigation.

Graphical Abstract

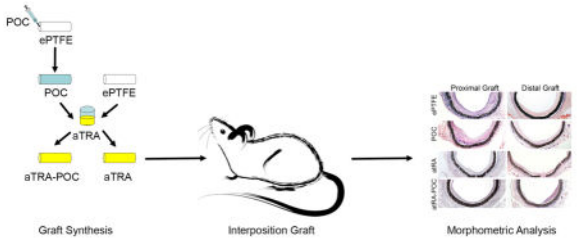

Keywords

Peripheral vascular disease; Restenosis; Intimal hyperplasia; atRA; endothelium; Nitric oxide

INTRODUCTION

Peripheral arterial disease is associated with significant morbidity and mortality, often necessitating vascular bypass grafting. Although great saphenous vein remains the gold standard conduit for small diameter bypass grafting, it is only suitable for use in one-third of the patient population.[1] The most commonly utilized prosthetic material, expanded polytetrafluoroethylene (ePTFE), continues to exhibit poor performance with 5-year primary patency rates for femoral below-the-knee popliteal and tibial artery targets of 43% and 22%, respectively.[2] There have been multiple prior approaches to improve ePTFE graft patency rates. Some of these strategies include: surgical modification to improve flow dynamics, alternative graft materials and coatings, and endoluminal modifications with proteins and drugs.[3] However, to date, a viable alternative has not made its way to the clinical area. Limitations of these modifications include no improvement in graft endothelialization or worsening of graft-artery compliance mismatch, leaving the exposed graft surface vulnerable to intimal formation. While there have been attempts to endothelialize grafts via 1- and 2-staged procedures, the success of these procedures has been limited due to the low density of endothelial cell seeding and the need for a 2-staged procedure, respectively.[3–5] Thus, the ideal graft modification should incorporate an agent that will promote graft endothelialization, not alter the physical properties of the graft, and inhibit intimal formation.

Retinoids are derivatives of vitamin A that occur in many isoforms. All-trans retinoic acid (atRA) is one isoform that has demonstrated versatile biological activities including: 1) involvement in embryogenesis, including vasculogenesis, 2) regulation of immune function and inflammation, and 3) effects on cell proliferation, differentiation, and migration.[6–8] Retinoids have classically been described to act on steroid nuclear receptor altering cellular transcription; however, retinoids can also influence signal transduction by activation of kinase cascades.[9] The utility of of atRA to inhibit intimal hyperplasia has been supported by numerous studies.[8–15] Several *in vitro* studies have demonstrated that atRA has favorable effects on vascular smooth muscle cells influencing their proliferation, differentiation, and migration.[8, 9, 11] Collectively these effects address the elements involved in the pathogenesis of intimal hyperplasia and arterial restenosis. Several *in vivo* studies have demonstrated that atRA not only inhibits intimal hyperplasia in various animal models, but also has been shown to accelerate reendothelialization after vascular injury.[10–15] While atRA is used clinically to treat a wide range of non-vascular human disease conditions, atRA has not been utilized clinically to treat vascular restenosis, despite the wide body of evidence in animal models demonstrating the efficacy of atRA to inhibit intimal formation.[13–15] The likely reason for this is that the dose required to achieve inhibition of intimal hyperplasia in animal studies is approximately 30-fold higher than the dose to treat cancer in humans.[14] Thus, a safer, more effective approach to atRA delivery is needed.

Unlike systemic diseases such as cancer, neointimal formation and restenosis are localized pathologies that are amenable to a localized therapy. Local delivery of atRA is expected to simplify delivery and significantly reduce the body's exposure to the drug, thereby avoiding off-target systemic effects. Thus, the objective of this research study was to assess if the incorporation of atRA into a standard ePTFE grafts would be effective at inhibiting intimal formation and/or accelerating graft endothelialization in a rat aortic interposition bypass model. We hypothesized that atRA- eluting ePTFE vascular grafts would be biocompatible, stimulate an endothelial cell monolayer, and inhibit intimal formation following bypass grafting. We also hypothesized that the surface atRA is immobilized onto (ePTFE vs POC) would impact the atRA loading and release profile and thus impact the efficacy of the graft to inhibit intimal hyperplasia. To test these hypotheses, atRA was immobilized via physisorption directly on the ePTFE vascular grafts or on POC-coated ePTFE vascular grafts. In this study we: 1) characterize the graft physical properties and the atRA loading and release profiles; 2) evaluate intimal formation and endothelialization of these grafts in a rat aortic bypass graft model; and 3) assess the safety and biocompatibility of these grafts.

Materials and Methods

Fabrication of POC-, atRA-, and atRA-POC-ePTFE grafts

POC-ePTFE, atRA-ePTFE and atRA-POC-ePTFE grafts were fabricated starting from standard ePTFE grafts (1.53 mm, IND 25 μM, wall thickness 100 μM, Zeus, Orangeburg, SC). Briefly, atRA-ePTFE was prepared by soaking ePTFE grafts in the dark for 24 hours in a 20 mg/mL solution of atRA (Sigma, St. Louis, MO) dissolved in dimethyl sulfoxide (Sigma, St. Louis, MO). To create POC-ePTFE grafts, POC pre-polymer was synthesized from equimolar amounts of citric acid and 1,8-octanediol. ePTFE grafts with the distal end

occluded were infused with a 30% (w/v) POC pre-polymer solution in ethanol until sweating of the grafts occurred, coating the entire luminal surface and wall thickness of the graft. The coated grafts were then post-polymerized at 80 C for 4 days, forming POC-ePTFE.[16, 17] Similar to atRA-ePTFE, atRA-POC-ePTFE grafts were prepared by soaking POC-ePTFE grafts in the dark for 24 hours in a 20 mg/mL solution of atRA (Sigma, St. Louis, MO) dissolved in dimethyl sulfoxide (Sigma, St. Louis, MO). Grafts were then rinsed with distilled water and lyophilized. All grafts were gas sterilized with ethylene oxide gas and soaked in DMEM cell culture media to leach out any acidic products. The DMEM was changed daily until no further DMEM discoloration was observed. The grafts were rinsed 3 times with phosphate buffered saline (PBS). Once prepared, the grafts were protected from light and stored at −20 C (Figure 1A).

In vitro characterization of POC-, atRA- and atRA-POC-ePTFE

3 mm sections from each graft were analyzed by scanning electron microscopy (SE, Hitachi 3500 N, EPIC, Northwestern University) to visualize atRA and POC loading. In addition, the endoluminal surface of 1 mm sections of graft divided lengthwise was evaluated utilizing Fourier transform infrared (FTIR) spectra in the attenuated total reflection mode, at room temperature using a Bruker Tensor II FTIR spectrometer (Billerica, MA) to further confirm atRA and POC loading. The elastic modulus for each graft type was assessed via radial compression. Briefly, 25 mm long graft sections were placed between two circular flat plates (2” diameter) attached to the InstronR Tester and the plates were advanced toward each other. All tests were performed on wetted graft samples. The force required to compress the graft radially from 0 to 0.8 mm (50%) was measured. Utilizing a similar method described by Gluhih et al., the compression data were utilized to calculate the elastic modulus for each of these materials. Briefly, the modulus for each point of compression was calculated utilizing the formula derived from the unified loading diagram, to determine the average modulus throughout the range of compression.[18]

Quantification of atRA loading and release profiles of atRA, 9-cis RA, and 13-cis RA release profiles

To quantify the amount of atRA loaded, 6 mm segment of grafts were washed 3 times with deionized water (500 ul/graft, 2 min), then air dried for 5 min. Grafts were then immersed in 1 ml of acetonitrile for 5 minutes to extract all the drug and the graft turned clear. The 1 ml of acetonitrile was evaluated using high performance liquid chromatography (HPLC) to determine that amount of atRA loaded. HPLC analysis was carried out using a Shimadzu HPLC system set at 35ºC with a SPD-20A diode array detector similar to published methods and the percent loading was calculated.[19] Samples of the were injected into an Ascentis RP-Amide column (150 mm × 2.1 mm, 3 μm particle size) (Sigma-Aldrich; St. Louis, MO). The solvent system consisted of HPLC-MS grade water (solvent A) and acetonitrile (solvent B) (each containing 0.1% (v/v) formic acid) with the following linear gradient at 400 μL/min: 0–3 minutes, hold at 70% B; 3–15 minutes, 70% B to 95% B; 15–20 minutes, hold at 95% B; 20–21 minutes, 95% B to 70% B; 21–26 minutes, re-equilibrate at 70% B. atRA was monitored using diode array detector set at 350 nm.[19] Quantification was based on the diode array peak area of retinoic acid and comparison to a standard curve of known concentration of atRA. To quantify the atRA release from all graft types, 6 mm sections of

graft were soaked in 48-well plates using 200 μL sterile LC/MS grade water at 37 C and protected from light. The water was collected and replaced daily for 32 days. The collected samples were lyophilized to recover any atRA released, dissolved in 100 μL acetonitrile, and quantified using HPLC as described previously. As atRA is known to isomerize to 9-cis RA and 13-cis RA, the release of all 3 isomers was quantified by the same method for each graft type. The amount of atRA released and the amount of atRA loaded at time of synthesis were used to calculate the percent atRA released.

Assessment of *in vitro* complement activation and platelet aggregation

Functional complement activation assays were performed on all grafts according to published methods.[19] Briefly, we utilized sheep red blood cells (RBC) obtained from whole blood (VWR, Chicago, IL) and human serum (Sigma, St. Louis, MO). Red blood cells were washed and sensitized with hemolysin diluted with PBS to the optimal concentration previously identified. 2×2 mm sections of graft material were incubated in serum (0.5 mg/ml and 1 mg/ml) at 37°C for 1 hour. After incubation, the serum was diluted to different concentrations and incubated with sensitized sheep RBC adjusted to 1.25×10^8 cells/ml) at 37°C for 1 hour. The samples were then read via plate reader at 412 nm to quantify the release of hemoglobin.

To evaluate platelet aggregation we utilized a method described by Messora et al.[20] Blood was collected from Sprague Dawley rats into citrate containing tubes. Platelet rich plasma (PRP) and platelet poor plasma (PPP) were isolated from these samples at room temperature via centrifugation of fresh blood at 150 g for 15 minutes (PRP) and 840 g for 20 minutes (PPP). The PRP was diluted with PPP to make a final platelet concentration between $2–3 \times 10^8$/ml. The platelet admixture was incubated with 2×2 mm sections of graft material at 37ºC for 15 minutes. The platelet suspension was aspirated and the grafts were rinsed 3 times with warmed PBS and transferred to a clean 96-well plate. The adherent platelets were then lysed using 100 μl of Triton-PBS. To quantify the platelets, lysates were quantified for the amount of lactate dehydrogenase read via plate reader at 650 nm.

Animal surgery

All animal procedures were performed in accordance with the Guide for the Care and Use of Laboratory Animals published by the National Institutes of Health (NIH Publication 85-23, 1996) and approved by the Northwestern University Animal Care and Use Committee. Twenty-eight 11-week-old male Sprague Dawley rats weighing between 350 and 400 g underwent an aortic interposition graft model as previously described.[21] Briefly, animals were anesthetized with isoflurane (1.5–5%) and treated preoperatively with carprofen subcutaneously (0.15 mg kg^{-1}) for pain control. Utilizing the Leica Wild M8 confocal microscope (Leica, Buffalo Grove, IL) via a midline incision the retroperitoneum was exposed and approximately 1.5 cm of the abdominal aorta was mobilized from the spermatic arteries to the aortic bifurcation. The left and right iliolumbar and/or the proximal lumbar arteries were ligated. Subcutaneous heparin (100 units/kg) was administered 20 minutes prior to cross clamping of the aorta. Once crossed clamped the aorta was transected 2–4 mm below the left iliolumbar artery. Proximal and distal anastomosis were constructed with 12 interrupted 9-0 nylon sutures (9-0 nylon BV130 needle, Suture express, Lenexa, KS). The

rectus abdominis muscle and skin were closed separately with a running 4-0 nylon suture. Groups included ePTFE, POC-ePTFE, atRA-ePTFE, and atRA-POC-ePTFE (n = 6–7 per treatment group).

Harvest and specimen processing

At 28 days, the animals were anesthetized as previously described and sacrificed via bilateral thoracotomy.[21] Blood was collected via cardiac puncture and the graft and 5 mm of native aorta proximal and distal to the anastomoses were harvested after *in situ* perfusion-fixation with PBS (500 mL) and 2% paraformaldehyde (500 mL) via the left ventricle. Once explanted the specimen was divided into proximal and distal segments and frozen in optimal cutting temperature compound using liquid nitrogen. The specimen blocks were cut into 5 μm sections. Each graft was analyzed at 4 regions including PA, PG, DG, and DA.

Morphometric analysis

Specimens were examined histologically for evidence of intimal formation utilizing 5-μm hematoxylin and eosin (H&E)-stained cross sections. Five to six equally-spaced sections from each of the 4 regions were stained from each animal. Digital images of stained sections were collected with light microscopy using a Zeiss Imager-A2 microscope (Hallbergmoos, Germany). At each location the luminal area, intimal area, medial area, and circumference were determined using ImageJ software (NIH; Bethesda, MD). In addition, when applicable, the intima-to-media area ratio (I/M), percent of the arterial wall composed of the intima (intimal area/intimal area + medial area or I/I+M), and percent stenosis (intima area/intimal area + lumen area * 100) were calculated.

Immunohistochemistry

To assess endothelialization and inflammation, for each animal 4 equally-spaced sections from the proximal and distal graft regions were stained with: CD31, a marker for endothelial cells; ED1, a marker for macrophages; or; CD45, a marker for leukocytes. Briefly, all sections were fixed as follows: CD31 and ED1 were fixed with 2% paraformaldehyde for 20 minutes at room temperature; CD45 sections were fixed with ice-cold acetone for 5 minutes. All sections were then rinsed with PBS for 2 minutes. CD45 and ED1 sections were permeabilized with 0.3% Triton X-100 in PBS, CD45 for 10 minutes and ED1 for 20 minutes. Sections were rinsed with PBS 2 minutes. Primary antibodies were applied as follows: CD31 (anti-CD31/PECAM/1 NOVUS, cat no. ab24590; Abcam, Cambridge, MA) diluted 1:500; CD45 (anti-Rat CD45, cat no. MCA43R, AbD serotec, Raleigh, NC) diluted 1:1000; ED1 (CD68, cat no. sc-59103; Santa Cruz Biotechnology, Santa Cruz, CA) diluted 1:50. All antibodies were diluted in immunohistochemistry-Tek (IHC-Tek diluent, pH 7.4, cat. no. 1W-1000; IHC World, Woodstock, MD). Specimens were incubated for 1 hour at room temperature and then rinsed with PBS for 2 minutes. The appropriate secondary antibodies (Invitrogen, Carlsbad, CA) were applied: Alexa Fluor 555, goat anti-rabbit IgG, 1:1000 dilution (cat. no. A-21429) for CD31; Alexa Fluor 555, goat anti-mouse IgG, 1:1000 dilution (cat. no. A-21424) for CD45; and Alexa Fluor 555, goat anti-mouse IgG, 1:500 dilution, (cat. no. A-21424) for ED1. All secondary antibodies were diluted with PBS and specimens were incubated for 1 hour at room temperature followed by a 2 minute PBS rinse. Nuclei were stained with DAPI in PBS (1:500, cat. no. D3571, Invitrogen) then rinsed in

sterile water and coverslipped with ProLongGold (cat. no. P36930, Invitrogen). For all stained sections, digital fluorescent images were acquired using Spot Advanced software (Diagnostic Instruments, Sterling Heights, MI) on a Nikon Eclipse 50i Microscope (Nikon Instruments, Melville, NY). The red staining was quantified for each graft section at four quadrants. Briefly, using ImageJ software (NIH) the area of red staining was quantitated for the intima (CD31) or the intima and graft (CD45, ED1). To quantitate the area of red staining the images were split into RGB-format, the green and blue images were subtracted from the red and the number of red pixels were quantified.

Statistical analysis

All results are expressed as mean ± standard error of the mean (SE). The difference between two groups was analyzed using Student's t-test while the differences between multiple groups were analyzed using one-way analysis of variance (ANOVA) with the Student-Newman-Keuls *post hoc* test to assess all pairwise comparisons, and for ANOVA on ranks the Dunn's Method was utilized (SigmaStat; SPSS, Chicago,IL). Statistical signi cance was assumed when $P \leq 0.05$.

RESULTS

Loading atRA onto ePTFE vascular grafts with or without POC did not significantly alter their microarchitecture or mechanical properties

Three grafts types were successfully fabricated: 1) poly(1,8 octamethylene citrate)-coated ePTFE (POC-ePTFE); 2) all-trans retinoic acid-coated ePTFE (atRA-ePTFE); and 3) all-trans retinoic acid coated onto POC-ePTFE (atRA-POC-ePTFE). A schematic of the preparation of atRA-POC-ePTFE is detailed in Figure 1A. ePTFE grafts served as controls for all experiments. Figure 1B depicts the scanning electron microscopy (SE) of the luminal surface of each graft (top) as well as the node and fibril structure of the different ePTFE grafts (bottom). Figure 1C–D summarizes the results of our compression testing to characterize the elastic modulus for each material. Using force to compress each graft from 0 to 0.8 mm, the plots of force versus compression resulted in lines with a classic toe region followed by a linear region from 0.4–0.6 mm. Analyzing these data via a method described by Gluhih et al. revealed an elastic modulus of 0.22, 0.14, 0.29, and 0.17 MPa for ePTFE, atRA-ePTFE, POC-ePTFE, atRA-POC-ePTFE, respectively.[18] In addition, comparison of the force required to compress the grafts by 25% and 50% revealed no significant differences between the grafts when compared to ePTFE controls (Figure 1C, P=NS)

atRA was successfully loaded onto atRA- and atRA-POC-ePTFE grafts with minimal isomerization and without activation of complement or platelet aggregation *in vitro*

Figure 2A–D show representative FTIR spectra for each graft denoting peaks specific to bonds for each material ePTFE, POC-ePTFE, atRA-ePTFE and atRA-POC. The carbon-fluorine bonds for ePTFE are present at 1200 (C–F symmetric stretch), 1150 (C–F asymmetric stretch) and 964 (CF_2 rocking). (Figure 2A–D). Figures 2B and 2D demonstrate methylene and ester carbonyl bonds found in POC with peaks at 2920 (CH_2-C), 2856 (CH_2-O) and 1734 (C=O). Alkene and ester carbonyl bond in atRA result in peaks at 2927 (=C-H, strong stretch), 1734 (C=O), 1576 (C=C) and 964 (=C-H, out of plane bending). While

peaks are present for atRA-POC-ePTFE (Figure 2D) only the peak at 964 was present for atRA-ePTFE (Figure 2C). Figure 2E–F summarizes changes in the FTIR spectra graft material from synthesis and after 30 days of soaking revealed little changes in spectra at 30 days for either graft type. While the atRA-ePTFE spectra only revealed a peak at 2927 (=C–H, strong stretch), the atRA-POC-ePTFE spectra revealed peaks at 2927 (=C–H, strong stretch) and 1734 (C=O). The presence of atRA on these grafts was further supported by HPLC. Table 1 summarizes the amount of atRA loaded onto each graft, with 5.9 μg of atRA loaded onto atRA-ePTFE and 103 μg onto atRA-POC-ePTFE. Next, we evaluated atRA release from the grafts for a period of 30 days. The chromatogram of a standard sample of retinoic acid (Figure 3A) demonstrated three peaks of similar amplitude at elution times specific for each isomer: 13-cis retinoic acid (13-cisRA, 10.84 minutes), 9-cis retinoic acid (9-cisRA, 11.59 minutes), and all-trans retinoic acid (atRA, 12.04 minutes). The superimposed chromatograms for the releasate collected from atRA-ePTFE and atRA-POC-ePTFE grafts revealed the most prevalent peak at 12.04 minutes, corresponding to the elution time for atRA (Figure 3A). Cumulative release of each isomer, atRA, 9-cisRA, and 13-cisRA was quantitated over 30 days for each graft type. All 3 isomers were released from the atRA-eluting ePTFE grafts (Figure 2A–D); however, atRA-POC-ePTFE resulted in significantly greater release of all 3 isoforms as compared to atRA-ePTFE. In particular, atRA release was 3.7-fold higher with atRA-POC-ePTFE as compared with atRA-ePTFE (Figure 3B, $P<0.05$). Table 1 summarizes the amount of atRA released after incubation for 30 days with the calculated percent released for each graft type. To assess biocompatibility of our material, we performed complement activation and platelet aggregation studies. No differences in complement activation or platelet aggregation were observed between POC-ePTFE, atRA-ePTFE, or atRA-POC-ePTFE grafts when compared to ePTFE grafts (Figure 3E–F, P=NS).

atRA-POC-ePTFE grafts exhibit reduced intimal hyperplasia, percent stenosis, and greater lumen area when compared to ePTFE grafts

After demonstrating successful atRA release and biocompatibility of the grafts *in vitro*, grafts were implanted as aortic interposition grafts in rats (Figure 4A). The distribution of intimal formation was assessed for each graft type after 4 weeks of implantation at the following areas: proximal artery (PA), proximal graft (PG), distal graft (DG) and distal artery (DA) (Table 2). For all 3 graft types the majority of the intimal formation was located at the graft anastomoses, with the intimal area at the PG being greater than the DG. Figure 4B–C demonstrates that the distribution of intimal formation for animals treated with ePTFE and POC-ePTFE was the same, with the proximal and distal graft sections exhibiting greater intimal area than both the proximal and distal arterial sections (*,**$P<0.05$). This pattern was altered in animals treated with the atRA-eluting ePTFE grafts. The intimal area at the DG was reduced in animals treated with atRA-ePTFE, thus only the intimal area at the PG was greater than the proximal and distal arterial segments. Similarly, treatment with atRA-POC-ePTFE reduced the intimal area at the PG and DG and the intimal area at the PG was only greater than the distal arterial segment (Figure 4D–E,†,†† $P<0.05$). Comparing the intimal formation at the proximal and distal graft sections for all treatment groups, animals treated with the atRA-ePTFE demonstrated a 48% reduction in intimal area at the DG as compared to those treated with the ePTFE grafts (Figure 5B). However, animals treated with

the atRA-POC-ePTFE demonstrated a 50% and 56% reduction in intimal area as compared to those treated with the ePTFE grafts at both the PG and DG respectively (Figure 5A–B, * P<0.05). Representative hematoxylin and eosin stained images are shown in Figure 5C. Other positive morphometric findings found in animals treated with either atRA-eluting ePTFE graft included an increase in medial and lumen areas and decrease in percent stenosis at both arterial and graft segments. However, only the animals treated with atRA-POC-ePTFE grafts demonstrated an increase in lumen area and decrease in percent stenosis at the PG, the site of the greatest intimal formation (Table 2).

atRA-POC-ePTFE grafts endothelialize more rapidly, are biocompatible, and do not elicit changes in liver and renal chemistries *in vivo*

As endothelialization greatly affects the degree of intimal formation, we investigated the differences in endothelialization of each graft type (Figure 6). Compared to ePTFE controls, animals treated with the atRA-POC-ePTFE graft demonstrated a 2.7-fold and 2.2-fold increase in graft endothelialization at the PG and DG, respectively (Figure 6A–B, *P<0.05). To further establish the biocompatibility of these grafts we assessed the inflammatory response to these materials *in vivo*, by examining the infiltration of macrophages (ED1) and total leukocytes (CD45) evoked by each graft type. Overall, we observed that most inflammatory cells were located in the graft material (Figure 7). At the proximal and distal graft sections, animals treated with atRA-POC-ePTFE grafts exhibited an 85% and 60% decrease in graft infiltration of ED1 and a 57% and 39% decrease in graft infiltration of CD45, respectively (*P<0.05). Lastly, to establish the biosafety profiles of these materials, liver and renal chemistries were analyzed on blood collected 30 days after implantation. No significant differences were observed among all groups (Table 3).

DISCUSSION

There is a clear need for new biomaterials and strategies to address the poor patency rates of currently available prosthetic vascular grafts. In this current study we investigate two strategies to prepare atRA-eluting ePTFE grafts: direct immobilization of atRA onto the ePTFE material (atRA-ePTFE) and atRA immobilization onto POC-coated ePTFE (atRA-POC-ePTFE). *In vitro* characterization revealed successful loading of POC-ePTFE, atRA-ePTFE, and atRA-POC-ePTFE with atRA release profiles demonstrating sustained atRA release with minimal isomerization to the 9- or 13-Cis-RA isomers with atRA-POC-ePTFE resulting in a 17.5 fold increase in atRA loading and a 4 fold increase of atRA release at 30 days when compared to atRA-ePTFE. The loading and release profiles of these materials were within the 100 μM range, previously demonstrated to be safe even under static conditions and several orders of magnitude less than is currently utilized clinically.[22, 23] Further evaluation of the *in vitro* biocompatibility of these materials revealed no changes in the platelet aggregation or complement activation. Utilizing a rat aortic interposition graft model, we observed the proximal neointimal growth is greater than the neointima observed in the distal graft. This finding differs from what is commonly found in human bypass grafting where the distal anastomosis results in greater restenotic lesion. However, our finding is in agreement with previous reports in murine models of interpositional graft.[24] Importantly, we demonstrated that treatment with atRA-ePTFE and atRA-POC-ePTFE

resulted in improvements in morphometric parameters including decreased intimal area, decreased percent stenosis, increased lumen, and medial areas. In addition, animals treated with the atRA-POC-ePTFE grafts demonstrated increased graft endothelialization, with a concomitant reduction in macrophage and leukocyte infiltration into the graft material. Finally, evaluation of hepato-renal chemistries at 30-days after implantation revealed no differences compared to ePTFE controls, suggesting that these modifications did not alter the biosafety of these materials.

The efficacy of atRA to inhibit intimal hyperplasia has been widely described in the literature.[12–15, 25, 26] Initial studies investigating atRA utilized balloon injury models. Initial studies by Miano and Derosa et al. demonstrated the efficacy of systemic delivery of atRA (5–25 mg/kg/day orally), using balloon injury models, reporting decreases in intimal area of 25–45% with favorable geometric remodeling, as evident by increased intima/media ratios, lumen area, and arterial circumference.[13, 14] Other investigators utilized a carotid interposition reversed vein bypass model to investigate the efficacy of orally delivered atRA (10 mg/kg/day) to inhibit intimal formation in a bypass setting. Initial investigations in this setting failed to show reduction in intimal area, but did report a reduction intimal thickness, increased medial area, and decreased intima/media ratio, which was encouraging.[10] However subsequent studies, utilizing a similar model reported that systemically delivered atRA decreased the proliferative index and increased the apoptotic index of graft neointimal cells.[11]

Later investigations investigated the efficacy of atRA to inhibit intimal formation when delivered locally.[25, 26] Initial investigations utilizing localized atRA delivery by Herdeg et al delivered 10 μM atRA endoluminally for 5 minutes failed to reveal significant decreases in intimal area.[25] Understanding that atRA delivery to the vasculature is effective, but depends on the route and concentration of delivery, our lab recently demonstrated that local delivery of atRA using a periadventitial membrane fabricated from POC resulted in a 56% decrease in intimal area and a reduction in intima/media area ratio and percent stenosis in a rat carotid balloon injury model.[26] Our current study supports these data by demonstrating that local delivery of atRA from atRA-eluting ePTFE grafts also reduces intimal area, percent stenosis, and increases lumen area and the inhibition of intimal formation that is comparable to reductions reported with studies utilizing other anti-proliferative agents such as rapamycin and paclitaxel coated ePTFE grafts.[22, 27]

Our in vivo findings are consistent with the effects that retinoids have been reported to exert on the vasculature and are likely being executed via the mechanisms previously described.[6, 8, 9, 11, 15, 28] It is accepted that retinoids exert their effects on the vasculature by binding steroid nuclear receptors Retinoic Acid Receptor (RAR) and Retinoic X Receptor (RXR), resulting in transcriptions of genes that regulate important cellular functions including proliferation, migration, differentiation, apoptosis and inflammation. Moreover, it has also been demonstrated that the effects of retinoids differ based on cell type and cell location (intima vs media).[6, 8, 9, 11, 15, 28] Rhee et al. reviews much of the relevant research that has been done to detail the complex mechanisms of action of retinoids on the vasculature in the setting of vascular injury and in the development of atherosclerosis. Briefly, previous work suggests that atRA inhibits neointimal hyperplasia by maintaining the differentiation

of medial VSMC, preventing their migration into the intima.[28] In addition, atRA inhibits the proliferation of intimal VSMC while simultaneously increasing the proliferation of endothelial cells and increasing their synthesis of nitric oxide (NO). The pleiotropic effects of retinoids on the cells of the vasculature might elucidate the advantages of their use over other antiproliferative agents previously investigated.[28]

Early research demonstrated that rapamycin and paclitaxel effectively inhibited intimal hyperplasia when incorporated into vascular stents. [29, 30] Therefore, subsequent studies examined the utility of these agents when incorporated into ePTFE.[22, 27] Cagiannos et al. utilized a porcine aortioiliac bypass model and demonstrated a 68% reduction in intimal hyperplasia but no change in graft endothelialization in animals treated with rapamycin coated ePTFE grafts.[22] Utilizing paclitaxel coated ePTFE grafts in a porcine arteriovenous bypass model, Lee et. al. demonstrated a 93% reduction in intimal area at the perianastomotic regions in a porcine arteriovenous graft model.[27] While these reductions of intimal formation are equal to or greater than the reduction we achieved with atRA-POC ePTFE, treatment with atRA has the benefit of increasing the rate of endothelialization, which was not reported with paclitaxel or rapamycin. In fact, clinically paclitaxel and rapamycin have been shown to have antiproliferative effects on both VSMC and endothelial cells. Thus, despite their efficacy to inhibit intimal hyperplasia, they have demonstrated a delay in endothelial healing when compared to bare metal stents.[29, 30] As intimal hyperplasia is a complex pathophysiological response to vascular injury, an agent that can offer selective effects on the proliferation of various cell types of the vasculature would be advantageous. Moreover, hastened endothelialization of the graft material supplies source of other vasoprotective molecules such as nitric oxide that act synergistically to further endothelization and inhibit intimal hyperplasia.

Given that intimal formation and long-term biocompatibility are greatly influenced by inflammation, we explored if atRA would exacerbate the inflammatory response to the graft material. The beneficial effects of atRA therapy on inflammation observed in this study was consistent with reports in prior publications.[7, 31] Zhang et. al. investigated the efficacy of systemic atRA to inhibit cardiac allograft vasculopathy in a rat abdominal heart transplant model and reported a 45% reduction in macrophage infiltration (CD68) with the addition of atRA (10 mg/kg/day orally) to the standard cyclosporine therapy.[7] Similarly, Kishimoto et al reported decreased macrophage infiltration (F4/80) in a ureteral obstruction model in animals treated with intraperitoneal injections of atRA 20 mg/kg/day.[32] In addition, our previous investigation of localized atRA delivery via atRA-POC periadventitial membranes found a similar decrease of 76% in macrophage infiltration (ED1) as demonstrated in our current study.[26] Thus, in addition to the favorable effects on the proliferation and migration of endothelial cells and VSMC, the anti-inflammatory effect of atRA-POC-ePTFE may also impact intimal formation and confirm the biocompatibility of this material.

Our study has limitations. While we demonstrated for the first time that localized atRA delivery was effective in inhibiting intimal formation in an aortic interposition graft model, we did not attempt to further elucidated the cellular mechanism for this finding. Given that the effects of atRA are complex, this initial study was to establish the feasibility of this technology based on mechanisms reported by us and other using different delivery methods.

Therefore, elucidation of the mechanism of action was outside the scope of this current investigation. Similarly, while we demonstrated that this decrease in intimal formation is associated with increased graft endothelialization, we did not identify the mechanism of increased endothelialization. Once established, EC can generate other vasoprotective molecules that may be acting synergistically to inhibit intimal formation. This may impact the application of our study to the clinical arena as there are three mechanisms of graft endothelialization -- trans-anastomotic, fall-out from circulating endothelial cells, and transmural migration -- only endothelial cell fall out and transmural migration have been reported to contribute to endothelialization of bypass grafts clinically.[33–35]

Another limitation of our study was that we did not pursue the differences in FTIR spectrum or difference in loading of atRA-ePTFE and atRA-POC-ePTFE. The presence of only some the atRA peaks on the atRA-ePTFE and atRA-POC ePTFE spectrum is most likely related to the small amount loaded onto the grafts, as confirmed by HPLC. Thus, this discrepancy most likely reflects limitation of detection by FTIR. The improvement in atRA loading is attributed to the increase of available surface areas as POC is deposited in the lumen and between the nodes and fibrils of the graft material.

Similarly, another limitation of our study is that we have not stablished the kinetic release pattern of atRA or identified the optimal dosage. This is important because unlike balloon angioplasty models, which simulate a time-limited injurious event to the vasculature, bypass grafting permanently alters the flow dynamics at the proximal and distal anastomosis generating a constant stimulus for endothelial cell dysfunction and intimal formation. Thus, to improve patency rates, sustained release of atRA is likely necessary and further investigation into the release characteristics and dosing of this agent in conjunction with POC and other viable polymer materials is warranted. Moreover, as with all initial animal studies, extrapolation of our results to the clinical arena may be limited for several reasons: 1) the rate of endothelialization is species-specific, 2) length of the conduits utilized are only a fraction of the length used clinically, 3) the duration of implantation is much shorter and 4) the flow dynamics differ greatly, lacking the distal atherosclerotic disease and resulting increased resistance seen clinically.[36] However, this work clearly demonstrates that the local delivery of atRA via direct immobilization onto a vascular graft can inhibit intimal formation while simultaneously increasing reendothelialization. Thus, future work should attempt to quantify release characteristics, the kinetic modeling of these grafts *in vivo*, and test different amounts of immobilized atRA to induce optimal inhibition of neointimal hyperplasia. In addition, further *in vivo* studies utilizing atRA-POC-ePTFE should be pursued in other animal models with similar vascular physiology to humans, utilizing longer graft segments, increased implantation times, and ideally under atherosclerotic conditions to further establish its clinical utility.

CONCLUSION

The findings of our current study showed that treatment with atRA-eluting ePTFE grafts significantly decreased intimal area with evidence of favorable remodeling, including increased lumen and medial areas and decreased percent stenosis. atRA-POC-ePTFE appeared to be more effective than atRA-ePTFE as it: 1) resulted in greater loading and

release of atRA *in vitro*, 2) had greater effect on intimal area, acting at both the proximal and distal graft segments 3) increased graft endothelialization, and 4) demonstrated greater inhibition of inflammation. These data strongly support the efficacy of atRA-POC ePTFE to inhibit intimal formation and hasten endothelialization that could potentially translate to improved patency and rate of prosthetic grafts as compared to traditional ePTFE grafts.

Acknowledgments

The authors would like to express their thanks to Lynnette Dangerfield for her administrative support.

GRANTS

This work was supported by funding from the National Institutes of Health (K08HL084203, MRK; T32 HL094293-01, EKG; 1R43HL096217-01A1), the Society for Vascular Surgery Foundation, the Northwestern Memorial Foundation Collaborative Development Initiative (the Center for Limb Preservation), and by the generosity of Mrs. Hilda Rosenbloom and Mrs. Eleanor Baldwin and the Northwestern University Dean's Contribution Fund.

References

1. Park KM, Kim YW, Yang SS, Kim DI. Comparisons between prosthetic vascular graft and saphenous vein graft in femoro-popliteal bypass. Ann Surg Treat Res. 2014; 87:35–40. [PubMed: 25025025]
2. Loh SA, Howell BS, Rockman CB, Cayne NS, Adelman MA, Gulkarov I, Veith FJ, Maldonado TS. Mid- and long-term results of the treatment of infrainguinal arterial occlusive disease with precuffed expanded polytetrafluoroethylene grafts compared with vein grafts. Ann Vasc Surg. 2013; 27:208–217. [PubMed: 22998787]
3. Kapadia MR, Popowich DA, Kibbe MR. Modified prosthetic vascular conduits. Circulation. 2008; 117:1873–1882. [PubMed: 18391121]
4. Dardik A, Liu A, Ballermann BJ. Chronic in vitro shear stress stimulates endothelial cell retention on prosthetic vascular grafts and reduces subsequent in vivo neointimal thickness. J Vasc Surg. 1999; 29:157–167. [PubMed: 9882800]
5. Kohler TR, Kirkman TR, Kraiss LW, Zierler BK, Clowes AW. Increased blood flow inhibits neointimal hyperplasia in endothelialized vascular grafts. Circ Res. 1991; 69:1557–1565. [PubMed: 1954675]
6. Bohnsack BL, Lai L, Dolle P, Hirschi KK. Signaling hierarchy downstream of retinoic acid that independently regulates vascular remodeling and endothelial cell proliferation. Genes Dev. 2004; 18:1345–1358. [PubMed: 15175265]
7. Zhang M, Wu Q, Shui C. All-trans retinoic acid attenuates cardiac allograft vasculopathy in rats. Transplant Proc. 2010; 42:1895–1898. [PubMed: 20620545]
8. Axel DI, Frigge A, Dittmann J, Runge H, Spyridopoulos I, Riessen R, Viebahn R, Karsch KR. All-trans retinoic acid regulates proliferation, migration, differentiation, and extracellular matrix turnover of human arterial smooth muscle cells. Cardiovasc Res. 2001; 49:851–862. [PubMed: 11230985]
9. Streb JW, Long X, Lee TH, Sun Q, Kitchen CM, Georger MA, Slivano OJ, Blaner WS, Carr DW, Gelman IH, Miano JM. Retinoid-induced expression and activity of an immediate early tumor suppressor gene in vascular smooth muscle cells. PLoS One. 2011; 6:e18538. [PubMed: 21483686]
10. Leville CD, Dassow MS, Seabrook GR, Jean-Claude JM, Towne JB, Cambria RA. All-trans-retinoic acid decreases vein graft intimal hyperplasia and matrix metalloproteinase activity in vivo. J Surg Res. 2000; 90:183–190. [PubMed: 10792961]
11. Leville CD, Osipov VO, Jean-Claude JM, Seabrook GR, Towne JB, Cambria RA. All-trans-retinoic acid decreases cell proliferation and increases apoptosis in an animal model of vein bypass grafting. Surgery. 2000; 128:178–184. [PubMed: 10922989]

12. Lee CW, Park SJ, Park SW, Kim JJ, Hong MK, Song JK. All-trans-retinoic acid attenuates neointima formation with acceleration of reendothelialization in balloon-injured rat aorta. J Korean Med Sci. 2000; 15:31–36. [PubMed: 10719805]
13. DeRose JJ, Madigan J, Umana JP, Prystowsky JH, Nowygrod R, Oz MC, Todd GJ. Retinoic acid suppresses intimal hyperplasia and prevents vessel remodeling following arterial injury. Cardiovascular Surgery. 1999; 7:633–639. [PubMed: 10519672]
14. Miano JM, Kelly LA, Artacho CA, Nuckolls TA, Piantedosi R, Blaner WS. all-Trans-retinoic acid reduces neointimal formation and promotes favorable geometric remodeling of the rat carotid artery after balloon withdrawal injury. Circulation. 1998; 98:1219–1227. [PubMed: 9743514]
15. Miano JM, Topouzis S, Majesky MW, Olson EN. Retinoid receptor expression and all-trans retinoic acid-mediated growth inhibition in vascular smooth muscle cells. Circulation. 1996; 93:1886–1895. [PubMed: 8635268]
16. van Lith R, Gregory EK, Yang J, Kibbe MR, Ameer GA. Engineering biodegradable polyester elastomers with antioxidant properties to attenuate oxidative stress in tissues. Biomaterials. 2014; 35:8113–8122. [PubMed: 24976244]
17. Hoshi RA, Van Lith R, Jen MC, Allen JB, Lapidos KA, Ameer G. The blood and vascular cell compatibility of heparin-modified ePTFE vascular grafts. Biomaterials. 2013; 34:30–41. [PubMed: 23069711]
18. Gluhih S, Kovalov A, Tishkunov A, Akishin P, Chate A, Auzins E, Kalnins M. Identification of the Elastic Modulus of Polymeric Materials by Using Thin-Walled Cylindrical Specimens. Mechanics of Composite Materials. 2012; 48:57–64.
19. A. F1984–99, Standard Practice for Testing for Whole Compelement Activation in Serum by Solid Materials, in.
20. Messora M, Nagata MJ, Furlaneto Flava, Dornelles RC, Bomfim SR, Deliberador TM, Garcia VG, Bosco AF. A standardized research protocol fo platelet-rich plasma (PRP) preparation in rats. RSBO. 2011; 8:299–304.
21. Gregory EK, Vercammen JM, Flynn ME, Kibbe MR. Establishment of a rat and guinea pig aortic interposition graft model reveals model specific patterns of intimal hyperplasia. J Vasc Surg. 2016
22. Cagiannos C, Abul-Khoudoud OR, DeRijk W, Shell DH, Jennings LK, Tolley EA, Handorf CR, Fabian TC. Rapamycin-coated expanded polytetrafluoroethylene bypass grafts exhibit decreased anastomotic neointimal hyperplasia in a porcine model. Journal of Vascular Surgery. 2005; 42:980–987. [PubMed: 16275457]
23. Douer D, Zickl LN, Schiffer CA, Appelbaum FR, Feusner JH, Shepherd L, Willman CL, Bloomfield CD, Paietta E, Gallagher RE, Park JH, Rowe JM, Wiernik PH, Tallman MS. All-trans retinoic acid and late relapses in acute promyelocytic leukemia: very long-term follow-up of the North American Intergroup Study I0129. Leuk Res. 2013; 37:795–801. [PubMed: 23528262]
24. Cooley BC. Mouse strain differential neointimal response in vein grafts and wire-injured arteries. Circ J. 2007; 71:1649–1652. [PubMed: 17895566]
25. Herdeg C, Oberhoff M, Baumbach A, Schroeder S, Leitritz M, Blattner A, Siegel-Axel DI, Meisner C, Karsch KR. Effects of local all-trans-retinoic acid delivery on experimental atherosclerosis in the rabbit carotid artery. Cardiovasc Res. 2003; 57:544–553. [PubMed: 12566127]
26. Gregory EK, Webb AR, Vercammen JM, Flynn ME, Ameer GA, Kibbe MR. Periadventitial atRA citrate-based polyester membranes reduce neointimal hyperplasia and restenosis after carotid injury in rats. Am J Physiol Heart Circ Physiol. 2014; 307:H1419–1429. [PubMed: 25239800]
27. Lee BH, Nam HY, Kwon T, Kim SJ, Kwon GY, Jeon HJ, Lim HJ, Lee WK, Park JS, Ko JY, Kim DJ. Paclitaxel-coated expanded polytetrafluoroethylene haemodialysis grafts inhibit neointimal hyperplasia in porcine model of graft stenosis. Nephrology Dialysis Transplantation. 2006; 21:2432–2438.
28. Rhee EJ, Nallamshetty S, Plutzky J. Retinoid metabolism and its effects on the vasculature. Biochim Biophys Acta. 2012; 1821:230–240. [PubMed: 21810483]
29. Yazdani SK, Farb A, Nakano M, Vorpahl M, Ladich E, Finn AV, Kolodgie FD, Virmani R. Pathology of drug-eluting versus bare-metal stents in saphenous vein bypass graft lesions. JACC Cardiovasc Interv. 2012; 5:666–674. [PubMed: 22721663]

30. Liuzzo JP, Ambrose JA, Coppola JT. Sirolimus- and taxol-eluting stents differ towards intimal hyperplasia and re-endothelialization. J Invasive Cardiol. 2005; 17:497–502. [PubMed: 16145242]
31. Stevison F, Jing J, Tripathy S, Isoherranen N. Role of Retinoic Acid-Metabolizing Cytochrome P450s, CYP26, in Inflammation and Cancer. Adv Pharmacol. 2015; 74:373–412. [PubMed: 26233912]
32. Kishimoto K, Kinoshita K, Hino S, Yano T, Nagare Y, Shimazu H, Nozaki Y, Sugiyama M, Ikoma S, Funauchi M. Therapeutic effect of retinoic acid on unilateral ureteral obstruction model. Nephron Exp Nephrol. 2011; 118:e69–78. [PubMed: 21228601]
33. Kidd KR, Patula VB, Williams SK. Accelerated endothelialization of interpositional 1-mm vascular grafts. J Surg Res. 2003; 113:234–242. [PubMed: 12957135]
34. Shi Q, Wu MH, Hayashida N, Wechezak AR, Clowes AW, Sauvage LR. Proof of fallout endothelialization of impervious Dacron grafts in the aorta and inferior vena cava of the dog. J Vasc Surg. 1994; 20:546–556. discussion 556–547. [PubMed: 7933256]
35. Pennel T, Zilla P, Bezuidenhout D. Differentiating transmural from transanastomotic prosthetic graft endothelialization through an isolation loop-graft model. J Vasc Surg. 2013; 58:1053–1061. [PubMed: 23541549]
36. Zilla P, Bezuidenhout D, Human P. Prosthetic vascular grafts: wrong models, wrong questions and no healing. Biomaterials. 2007; 28:5009–5027. [PubMed: 17688939]

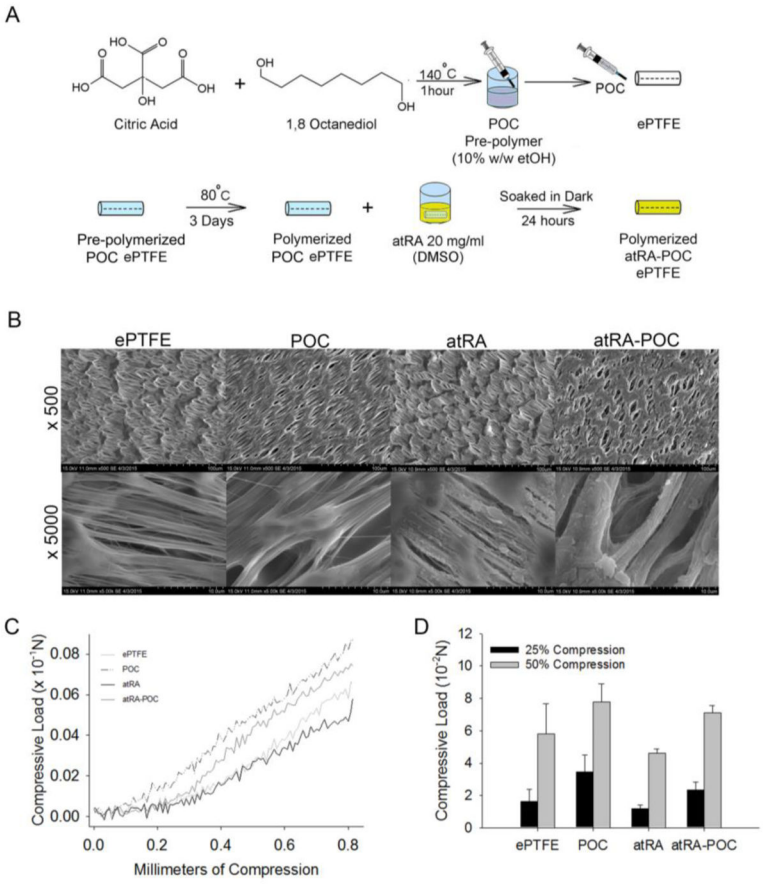

Figure 1. Synthesis and *in vitro* characterization of ePTFE, POC-ePTFE, atRA-ePTFE, and atRA-POC-ePTFE

(A) Schematic of atRA-POC-ePTFE synthesis. (B) Scanning electron microscopy image of the luminal surface of ePTFE, POC-ePTFE, atRA-ePTFE and atRA-POC-ePTFE demonstrating the node and fibril structure. (C) Mechanical testing of the grafts via radial compression measurements. (D) Quantification of force required to compress each graft to 25 and 50%. Data represent the mean ± SE (n=3), analysis via one-way ANOVA. Scale bar = 20 μm, original magnification = 2.0k. ePTFE: extended polytetrafluroethylene, POC-ePTFE: poly(1,8 octamethylene citrate) ePTFE, atRA-ePTFE: all-trans retinoic acid-coated ePTFE, and atRA-POC-ePTFE: all-trans retinoic acid- poly(1,8 octamethylene citrate) ePTFE.

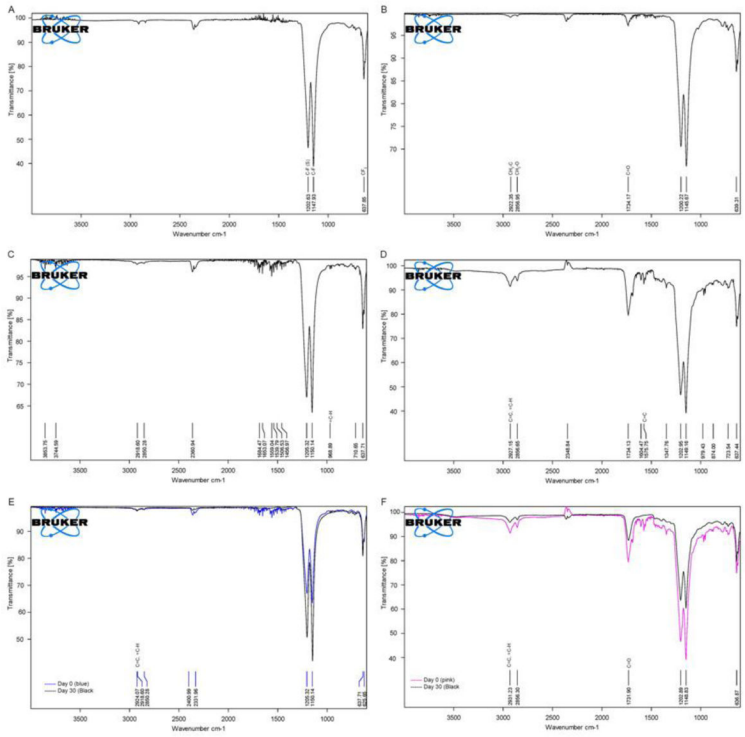

Figure 2. FTIR spectra of ePTFE, POC-ePTFE, atRA-ePTFE, and atRA-POC-ePTFE

Representative FTIR spectrum indicating characteristic peaks for each graft after synthesis and after 30 day release (A) ePTFE. (B) POC-ePTFE. (C) atRA-ePTFE and (D) atRA-POC-ePTFE. (E) atR-ePTFE at 0 and after 30 day release. (F) atRA-POC-ePTFE at 0 and after 30 day release. FTIR: Fourier transform infrared, ePTFE: extended polytetrafluroethylenePOC-ePTFE: poly(1,8 octamethylene citrate) ePTFE, atRA-ePTFE: all-trans retinoic acid-coated ePTFE, and atRA-POC-ePTFE: all-trans retinoic acid- poly(1,8 octamethylene citrate) ePTFE

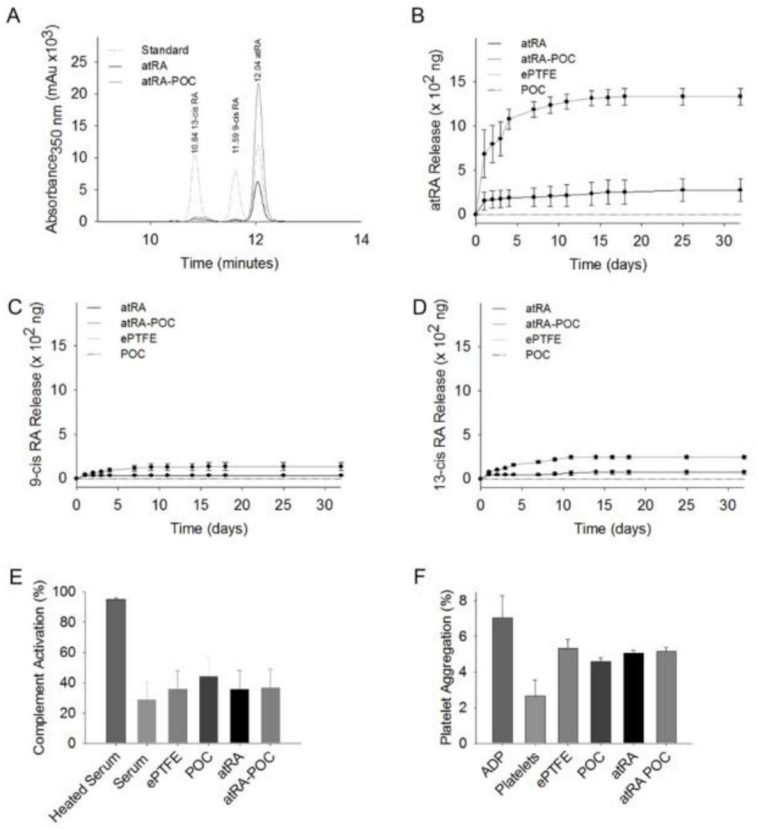

Figure 3. atRA-ePTFE and atRA-POC-ePTFE exhibit sustained release of atRA for 30 days and are biocompatible *in vitro*

(A) Representative high performance chromatography (HPLC) performed on samples of retinoic acid (RA, standard), and releasate from atRA-ePTFE and atRA-POC-ePTFE. (B–D) Quantification of the isoforms of RA released from ePTFE, POC-ePTFE, atRA-ePTFE, and atRA-POC-ePTFE grafts including: (B) atRA, (C) 9-cis RA, and (D) 13-cis RA over 32 days. (E) Assessment of the percent complement activation elicited by POC-ePTFE, atRA-ePTFE, atRA-POC-ePTFE grafts as compared with ePTFE alone. (F) Assessment of the percent platelet aggregation elicited by POC-ePTFE, atRA-ePTFE, and atRA-POC-ePTFE as compared with ePTFE alone. ADP (100 μM). Data represent the mean ± SE (n=3), analysis via one-way ANOVA. ePTFE: extended polytetrafluroethylene, POC-ePTFE: poly(1,8 octamethylene citrate) ePTFE, atRA-ePTFE: all-trans retinoic acid-coated ePTFE, and atRA-POC-ePTFE: all-trans retinoic acid- poly(1,8 octamethylene citrate) ePTFE

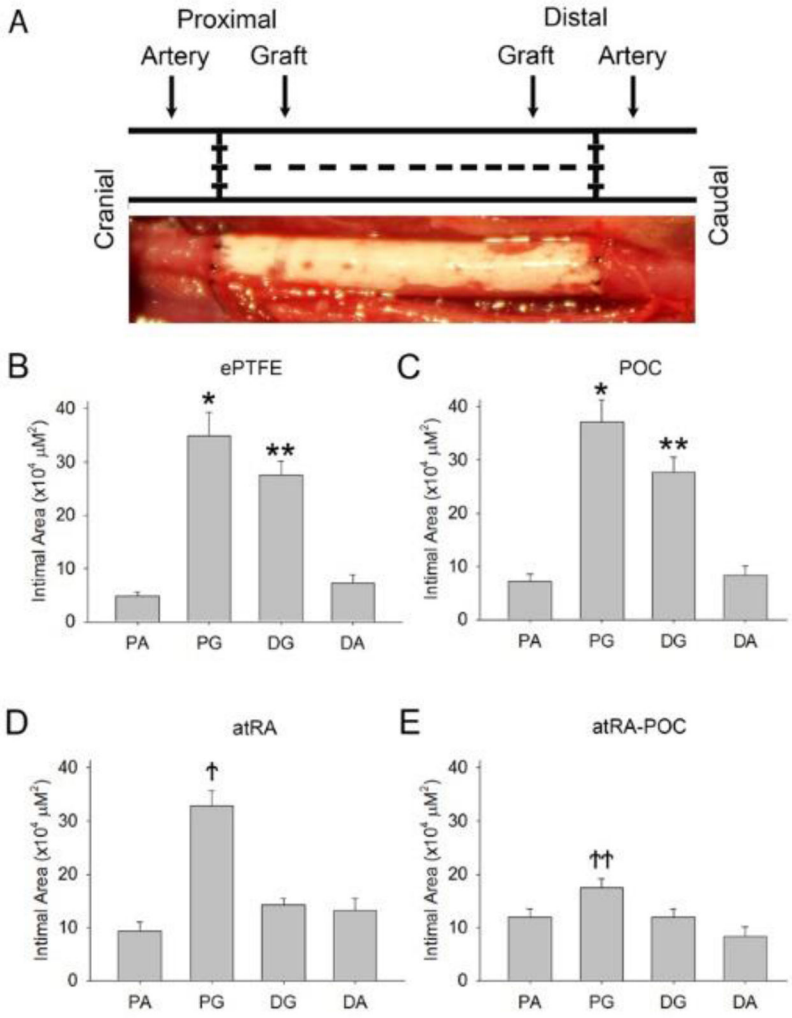

Figure 4. Grafts containing atRA exhibit an altered distribution of intimal formation

(A) Schematic of sample processing, and representative harvested sample. (B–E) Quantification of intimal area at all 4 regions: proximal artery, proximal graft, distal graft, and distal artery for (B) ePTFE, (C) POC-ePTFE, (D) atRA-ePTFE and (E) atRA-POC-ePTFE grafts. Data expressed as mean ± SE, represents 5–6 sections at each location from each rat (n=6–7/treatment group), analysis via one-way ANOVA. *$P < 0.05$ and **$P < 0.05$ versus PA and DA; ↑$P < 0.05$ versus PA, DG and DA; ↑↑$P < 0.05$ versus DA. PA: proximal artery, PG: proximal graft, DG: distal graft, DA: distal artery, ePTFE: extended polytetrafluroethylene, POC-ePTFE: poly(1,8 octamethylene citrate) ePTFE, atRA-ePTFE: all-trans retinoic acid-coated ePTFE, and atRA-POC-ePTFE: all-trans retinoic acid- poly(1,8 octamethylene citrate) ePTFE.

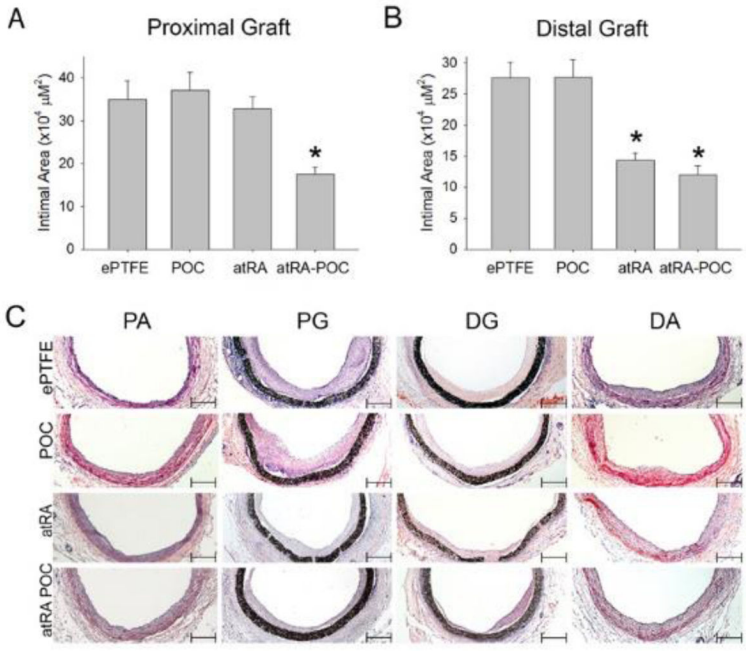

Figure 5. Grafts containing atRA exhibited decreased intimal area at the proximal and distal ends of the graft

(A–B) Quantification of the intimal area at the (A) proximal graft (PG) and (B) distal graft (DG). (C) Representative cross sections used to perform morphometric analysis for each graft and region. Data expressed as mean ± SE, represents 5–6 sections at each region for each rat (n=6–7/treatment group), analysis via one-way ANOVA. *P < 0.05 versus ePTFE. Scale bar = 50 μm, original magnification = x 2.5. PG: proximal graft, DG: distal graft, ePTFE: extended polytetrafluroethylene, POC-ePTFE: poly(1,8 octamethylene citrate) ePTFE, atRA-ePTFE: all-trans retinoic acid-coated ePTFE, and atRA-POC-ePTFE: all-trans retinoic acid- poly(1,8 octamethylene citrate) ePTFE.

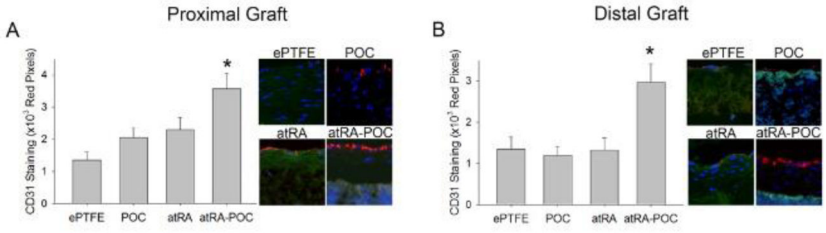

Figure 6. atRA-POC-ePTFE grafts exhibited increased graft endothelialization

(A–B) Representative CD31 staining (red) of graft cross section and quantification of staining for the (A) proximal graft and (B) distal graft. Blue = nuclei stained with DAPI; red = endothelial cells; and green = autofluorescence. Data expressed as mean ± SE, represents 4–5 sections at each region for each rat (n=6–7/treatment group), analysis via one-way ANOVA. *P < 0.05 versus ePTFE. Original magnification = x 2.5, quadrants = x 20. PG: proximal graft, DG: distal graft, ePTFE: extended polytetrafluroethylene, POC-ePTFE: poly(1,8 octamethylene citrate) ePTFE, atRA-ePTFE: all-trans retinoic acid-coated ePTFE, and atRA-POC-ePTFE: all-trans retinoic acid- poly(1,8 octamethylene citrate) ePTFE.

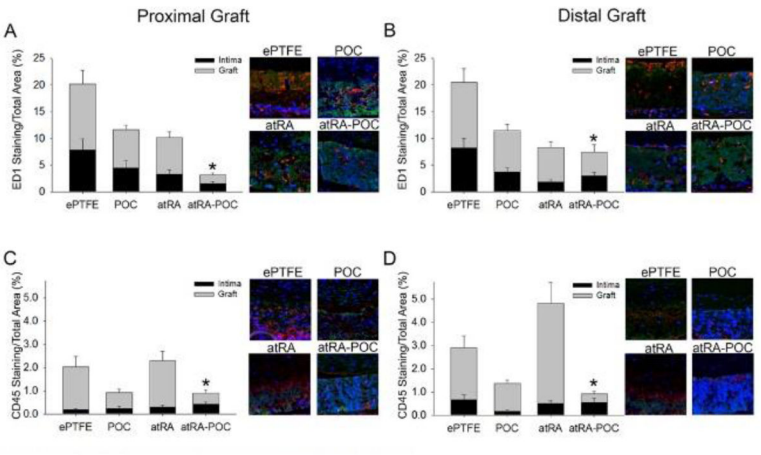

Figure 7. atRA-POC-ePTFE grafts exhibited decreased macrophage (ED1) and leukocyte (CD45) infiltration

(A–D) Representative cross sections and quantification of staining in the intimal and graft layers for: (A–B) ED1 staining (red), and (C–D) CD45 staining (red) at the (A,C) proximal graft and (B,D) distal graft regions. Blue = nuclei stained with DAPI; red = ED1 or CD45 staining; and green = autofluorescence. Data expressed as mean ± SE, represents 4–5 sections at each region for each rat (n=6–7/treatment group), analysis via one-way ANOVA. *P < 0.05 versus ePTFE. Original magnification = x 2.5, quadrants = x 10. PG: proximal graft, DG: distal graft, ePTFE: extended polytetrafluroethylene, POC-ePTFE: poly(1,8 octamethylene citrate) ePTFE, atRA-ePTFE: all-trans retinoic acid-coated ePTFE, and atRA-POC-ePTFE: all-trans retinoic acid- poly(1,8 octamethylene citrate) ePTFE.

Table 1

atRA and percent release at 30 days.

Graft	atRA loading per graft (μg)	atRA release 30 days (μg)	Percent atRA release 30 days (%)
atRA	5.9 ± 1.2	0.70 ± 0.02	3.00 ± 0.01
atRA-POC	103.3 ± 8.7	3.1 ± 0.3	11.20 ± 0.03

% 30 day release = (30 day release mass / loading total) * 100)

Table 2

Morphometric Analysis 28 Days after Implantation.

Location/Graft	Circumference Mean ± SE × 10^2	Lumen Area Mean ± SE × 10^5	Intimal Area Mean ± SE × 10^5	Percent Stenosis Mean ± SE	Medial Area Mean ± SE × 10^5	I/M Mean ± SE	I/(I+M) Mean ± SE
Proximal Artery							
ePTFE	12.2 ± 0.6	9.6 ± 0.7	0.49 ± 0.7	5.0 ± 0.7	2.2 ± 0.2	0.18 ± 0.03	0.15 ± 0.18
POC	13.3 ± 0.6	10.3 ± 0.7	0.72 ± 1.3	5.5 ± 1.1	2.8 ± 0.1	0.25 ± 0.05	0.17 ± 0.19
atRA	15.4 ± 0.5	11.1 ± 0.4	0.94 ± 1.6	7.2 ± 1.0	3.4* ± 0.1	0.22 ± 0.03	0.20 ± 0.03
atRA-POC	16.8 ± 0.4	12.2* ± 0.3	0.89 ± 1.6	6.3 ± 0.9	3.8* ± 1.3	0.25 ± 0.22	0.12 ± 0.02
Proximal Graft							
ePTFE	26.5 ±1.1	16.3 ± 0.5	3.49 ± 4.4	16.2 ± 1.3	-	-	-
POC	30.6 ± 0.8	22.5 ± 1.5	3.71 ± 4.2	14.3 ± 1.4	-	-	-
atRA	31.4 ± 3.4	21.2 ± 1.4	3.28 ± 2.8	6.2 ± 1.0	-	-	-
atRA-POC	26.3 ± 0.6	26.3* ± 0.3	1.75* ± 1.6	8.8* ± 0.8	-	-	-
Distal Graft							
ePTFE	30.3 ± 1.2	21.1 ± 1.1	2.76 ± 2.5	11.9 ± 1.2	-	-	-
POC	30.9 ± 0.9	21.4 ± 0.7	2.76 ± 2.8	11.1 ± 1.0	-	-	-
atRA	29.6 ± 1.5	21.8 ± 1.4	1.43* ± 1.2	7.3* ± 0.7	-	-	-
atRA-POC	26.3 ± 0.5	19.2 ± 0.4	1.20* ± 1.4	5.8* ± 0.7	-	-	-
Distal Artery							
ePTFE	11.4 ± 0.6	8.2 ± 0.5	0.73 ± 1.5	7.6 ± 1.4	2.4 ± 1.2	0.31 ± 0.07	0.20 ± 0.03
POC	12.5 ± 0.6	8.7 ± 0.3	0.84 ± 1.6	7.7 ± 1.1	2.8 ± 0.9	0.22 ± 0.03	0.18 ± 0.02
atRA	15.8 ± 0.6	11.9* ± 1.0	1.32 ± 2.2	9.2 ± 1.2	3.6* ± 2.2	0.25 ± 0.05	0.20 ± 0.03
atRA-POC	16.3 ± 0.7	12.1* ± 0.5	0.83 ± 1.8	5.8 ± 1.1	3.4* ± 1.2	0.25 ± 0.05	0.18 ± 0.02

*P<0.05 compared to ePTFE;

"-" Not Applicable since there is no media in the graft

Table 3

Liver and Renal Chemistries 30 Days after Implantation

Lab Test	Control		ePTFE		POC		atRA		atRA-POC	
	Mean	±SEM	Mean	±SEM	Mean	±SEM	Mean	±SEM	Mean	±SEM
Alkaline Phosphatase (U/L)	185	±19	155	±15	166	±17	183	±20	154	±18
Alanine transaminase (U/L)	94	±13	18	±9	58	±17	66	±11	64	±8
Aspartate transaminase (U/L)	145	±27	136	±49	117	±17	114	±11	97	±9
Creatine phosphokinase (U/L)	565	±118	317	±60	265	±46	241	±42	306	±16
Tot Protein (g/L)	5.5	±0.1	4.9	±0.2	5.0	±0.3	5.3	±0.4	5.0	±0.2
Albumin (g/L)	2.9	±0.10	2.4	±0.09	2.4	±0.20	2.5	±0.19	2.5	±0.10
Cholesterol (mg/dL)	86.5	±5.0	70.3	±5.7	75.3	±9.7	85.3	±16.3	34.5	±13.5
Blood urea nitrogen (mg/dL)	18	±1	20.5	±0.5	19.5	±0.6	19.3	±0.7	21.3	±0.8
Creatinine (mg/dL)	0.40	±0.02	0.63	±0.03	0.5	±0.09	0.50	±0.06	0.50	±0.04
Phosphate (mg/dL)	7.3	±0.2	8.5	±0.14	7.3	±0.50	6.8	±0.31	7.2	±0.45
Bicarbonate (mEq/L)	25.8	±0.5	17.3	±1.7	22.5	±1.9	20.7	±2.0	20.6	±2.4
Sodium:potassium ratio	31	±0.7	34.3	±5.8	28.8	±2.3	33.3	±4.0	33.0	±4.4